

Linear magnetoresistance in HgTe quantum wells

G. M. Gusev,¹ E. B. Olshanetsky,² Z. D. Kvon,^{2,3} N. N. Mikhailov,² and S. A. Dvoretzky²

¹*Departamento de Física dos Materiais e Mecânica, Instituto de Física da Universidade de São Paulo, 135960-170, São Paulo, SP, Brazil*

²*Institute of Semiconductor Physics, Novosibirsk 630090, Russia*

³*Novosibirsk State University, Novosibirsk, 630090, Russia*

(Received 15 January 2013; published 25 February 2013)

We report magnetotransport measurements in a HgTe quantum well with an inverted band structure, which is expected to be a two-dimensional (2D) topological insulator. A small magnetic field perpendicular the 2D layer breaks the time-reversal symmetry and thereby suppresses the edge state transport. A linear magnetoresistance is observed in low magnetic fields when the chemical potential moves through the bulk gap. That magnetoresistance is well described by numerical calculations of the edge state magnetotransport in the presence of nonmagnetic disorder. With the magnetic field increasing, both the local and nonlocal resistances first sharply decrease and then increase again in disagreement with the existing theories.

DOI: [10.1103/PhysRevB.87.081311](https://doi.org/10.1103/PhysRevB.87.081311)

PACS number(s): 73.43.Qt, 72.20.My, 72.25.Dc

Topological insulators are a novel type of system with a gap in the energy spectrum of the bulk states and a gapless energy spectrum of a special class of electron states located at their surface or edges.^{1–3} The two-dimensional (2D) topological insulator (TI) has gapless states propagating along its edges.^{4,5} There are two famous examples of such a system: the quantum Hall effect (QHE) state, which exists in a strong magnetic field perpendicular to the plane and is characterized by chiral edge states, and the time-reversal symmetric quantum spin Hall effect (QSHE) state, which is induced by a strong spin-orbit interaction and is characterized by counterpropagating states with opposite spins in the absence of magnetic field.

The QSHE has been realized in HgTe/CdTe quantum wells with an inverted band structure.^{6,7} The existence of edge channel transport in the QSH regime has been proved experimentally⁴ when a four-probe resistance in a HgTe/CdTe micrometer-sized ballistic Hall bar demonstrated a quantized plateau $R_{xx} \simeq h/2e^2$. Additional experimental evidence for edge states in the QSHE is nonlocal transport since the application of the current between any pair of probes creates a net current along the sample edge and can be detected by any other pair of voltage probes.^{8,9} It is expected that the stability of helical edge states in the topological insulator is unaffected by the presence of weak disorder.^{1,3,10–14} Note, however, that the quantized ballistic transport has been observed only in micrometer-sized samples and the plateau $R_{xx} \simeq h/2e^2$ is destroyed if the sample size is above a certain critical value of about a few microns.⁴

A magnetic field perpendicular to the 2D layer breaks time-reversal symmetry (TRS) and thereby enables elastic scattering between counterpropagating chiral edge states. However, a number of different theoretical models have previously been proposed^{4,15–18} and conflicting scenarios have been developed for TRS breaking in the QHSE system, which requires detailed experimental investigation.

A sharp magnetoresistance spike has been observed in the previous study of a HgTe-based sample a few microns in size.⁴ Nevertheless, it is very likely that these experiments have been done in the regime where the disorder strength W is of the same order as or even larger than the bulk energy gap E_g . In this paper we report on the observation and a systematic

investigation of a positive linear magnetoresistance in HgTe quantum wells with an inverted band structure corresponding to the QSHE phase. The magnetoresistance in low fields is described by a theoretical model¹⁸ that takes into account the combined effect of disorder and TRS breaking in a weak disorder regime where $W < E_g$. In magnetic fields above 2 T we observe a decrease of the resistance with saturation, corresponding to the QHE phase, followed by a transition to a state with a higher resistance and nonlocal transport in fields above 6 T.

The Cd_{0.65}Hg_{0.35}Te/HgTe/Cd_{0.65}Hg_{0.35}Te quantum wells with (013) surface orientations and a width d of 8–8.3 nm were prepared by molecular beam epitaxy. A detailed description of the sample structure has been given in Refs. 19–21. The six-probe Hall bar was fabricated with a lithographic length of 6 μm and a width of 5 μm (Fig. 1, inset). The ohmic contacts to the two-dimensional gas were formed by the in-burning of indium. To prepare the gate, a dielectric layer containing 100 nm of SiO₂ and 200 nm of Si₃Ni₄ was first grown on the structure using the plasmochemical method. Then a TiAu gate of size 18 \times 10 μm^2 was deposited. Several devices with the same configuration have been studied. The density variation with the gate voltage was $1.09 \times 10^{15} \text{ m}^{-2} \text{ V}^{-1}$. The magnetotransport measurements in the described structures were performed in the temperature range 1.4–25 K and in magnetic fields up to 12 T using a standard four-point circuit with a 3–13 Hz ac current of 0.1–10 nA through the sample, which is sufficiently low to avoid overheating effects.

The carriers density in HgTe quantum wells can be varied electrostatically with the gate voltage V_g . The typical dependence of the four-terminal $R_{xx} = R_{I=1,4;V=2,3}$ and Hall $R_{xy} = R_{I=1,4;V=3,5}$ resistances of one representative sample as a function of V_g is shown in Fig. 1(a). The resistance R_{xx} exhibits a sharp peak that is ~ 20 times greater than the universal value $h/2e^2$, which is expected for the QSHE phase. This value varies from 150 to 300 k Ω in different samples. The Hall coefficient reverses its sign and $R_{xy} \approx 0$ when R_{xx} approaches its maximum value,⁹ which can be identified as the charge neutrality point (CNP). This behavior resembles the ambipolar field effect observed in graphene.²² The gate voltage induces charge density variations, transforming the

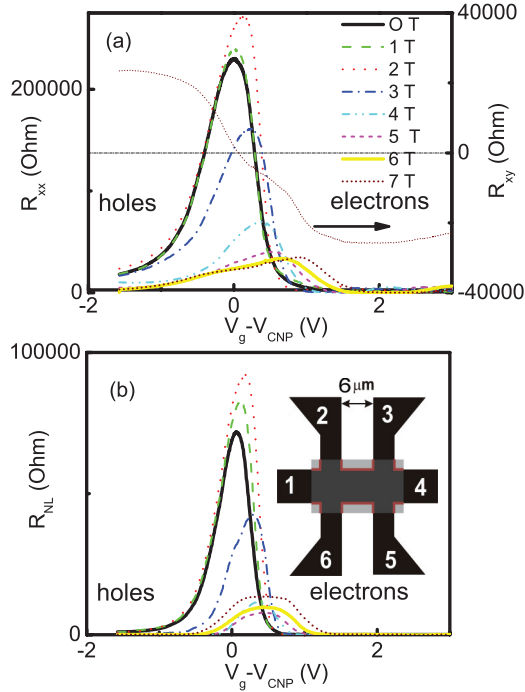


FIG. 1. (Color online) (a) Longitudinal R_{xx} ($I = 1,4$; $V = 2,3$) and Hall R_{xy} ($I = 1,4$; $V = 3,5$) resistances as a function of the gate voltage at zero and different nonzero magnetic fields, with $T = 4.2$ K. (b) Nonlocal R_{NL} ($I = 1,2$; $V = 3,5$) resistance as a function of the gate voltage at zero and different nonzero magnetic fields. The inset (b) shows the top view of the sample. The gate is shown by a rectangle.

quantum well conductivity from n type to p type via a QHSE state.

As we mentioned above, the edge state transport is unaffected by the presence of weak disorder.^{1,3,10–14} However, the quantized ballistic transport and plateau $R_{xx} \approx h/2e^2$ have not been observed in samples with dimensions above a few microns.⁴ One possible explanation is the presence of local fluctuations of the energy gap induced by smooth inhomogeneities, which can be represented as metallic islands. In accordance with the Landauer-Büttiker formalism,²³ any voltage probe coupled to a coherent conductor introduces incoherent inelastic processes and modifies the ballistic transport. Metallic islands can result in similar effects since an electron entering the island is dissipated and thermalized there and later on fed back into the system. Therefore, ballistic coherent transport is expected only in the region between the islands and the total four-terminal resistance exceeds the quantized value. However, such long-range potential fluctuations must have the amplitude of the order of the energy gap $E_g \sim 30$ meV, which is very unlikely since such fluctuations should suppress the electron SdH oscillations in low magnetic fields, which is not observed in the experiment. The resistance of samples longer than $1 \mu\text{m}$ might be much higher than $h/2e^2$ due to the presence of the spin dephasing (electron-spin-flip backscattering on each boundary).²⁴ Mechanisms of backscattering are new and appealing tasks for theoreticians and are a matter of ongoing debate. The classical and quantum magnetic impurities may introduce a backscattering between counterpropagating channels. An accidentally formed quantum

dot with an odd number of trapped electrons could play a role in such magnetic impurity. For a strong enough electron-electron interaction the formation of a Luttinger liquid insulator with a thermally activated transport was predicted.²⁵ In the framework of a somewhat different approach, an edge state transport theory in the presence of spin-orbit Rashba coupling has been developed.²⁶ According to this model, the combination of a spatially nonuniform Rashba spin-orbit interaction and a strong electron-electron interaction leads to localization of the edge electrons at low temperatures. However, an exact examination and a comparison with theoretical models require further experimental investigation of the temperature, doping, and disorder dependence of the resistivity, which is beyond the scope of the present paper.

Figure 1(b) shows the nonlocal resistance R_{NL} corresponding to the configuration where the current flows between contacts 1 and 2 and the voltage is measured between contacts 3 and 5. One can see that the nonlocal resistance $R_{NL} = R_{I=1,2;V=3,5}$ in the topological insulator phase has a peak of a comparable amplitude, though less wide, and approximately in the same position as the local resistance. Outside the peak the nonlocal resistance is negligible. The evolution of resistances with magnetic field is practically the same in both cases: Resistance grows with field below 2 T and then rapidly decreases and saturates. Figure 2 shows the longitudinal resistance R_{xx} in the voltage–magnetic-field plane. One can see the evolution of the resistance R_{xx} with magnetic field and density when the chemical potential crosses the bulk gap. The magnetoresistance demonstrates a striking V-shape dependence in magnetic fields below 1 T. It is worth noting that the V-shaped magnetoresistance is observed almost anywhere on the hole side of the peak and rapidly disappears on the electronic side.

In magnetic fields above 2 T the magnetoresistance starts to decrease, marking a pronounced crossover to the quantum Hall effect regime. Note, however, that the resistance does not turn to zero, as would be expected for a conventional QHE state, but approaches the value $R_{xx} \approx h/e^2$. Figure 3 shows the magnetic-field dependence extended to 12 T of the local

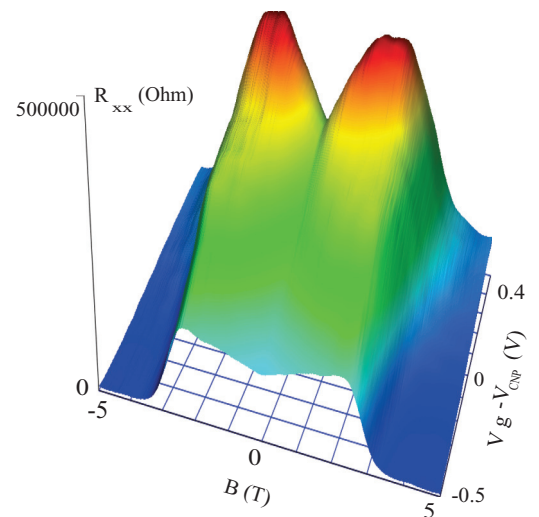


FIG. 2. (Color online) Longitudinal resistance R_{xx} as a function of the gate voltage and magnetic field, with $T = 1.4$ K.

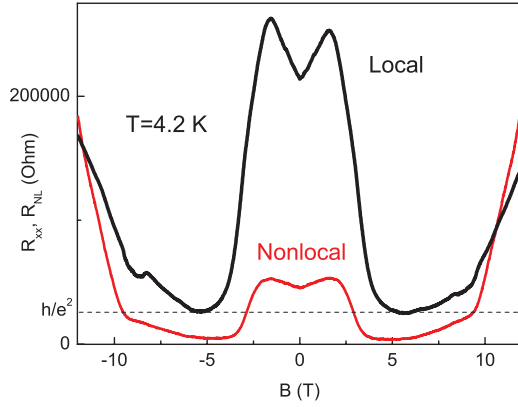


FIG. 3. (Color online) Local R_{xx} and nonlocal $R_{NL} = R_{I=2,6;V=3,5}$ resistances as a function of the magnetic field near the peak maximum (CNP), with $T = 4.2$ K.

and nonlocal resistances at the gate voltage corresponding the peak maximum for another representative sample. Both the local and nonlocal resistances grow rapidly in fields above 6 T. The evolution of the magnetoresistance in a strong quantized magnetic field disagrees with the theoretical models proposed recently for transport in HgTe quantum wells with an inverted band structure.^{16,17} The growth of the local and nonlocal resistances in the field above 6 T can be attributed to the edge state transport via counterpropagating chiral modes similar to the HgTe semimetal²⁷ and graphene²⁸ near $\nu = 0$. Further theoretical work would be needed to explain this behavior.

Figure 4 shows the low-field part of the relative magnetoconductivity $\sigma_{xx}(B)/\sigma_{xx}(0)$ for two values of the gate voltage, one at the CNP and the other just slightly below the CNP on the electron side of the TI peak. The conductivities have been recalculated from experimentally measured ρ_{xx} and ρ_{xy} by tensor inversion. Note, however, that around the CNP $\rho_{xy} \ll \rho_{xx}$ and $\sigma_{xx} \approx 1/\rho_{xx}$.

One can see that the low-field part of the conductivity is describe by the linear function $\sigma_{xx}(B)/\sigma_{xx}(0) = -\alpha|B|$, where the parameter $\alpha \approx d[\sigma_{xx}(B)/\sigma_{xx}(0)]/dB$ is slightly dependent on temperature and gate voltage [Fig. 4(c)]. It is worth noting that in a small region around zero the magnetoconductance shows a parabolic behavior.

In the rest of the paper we will focus on the explanation of the cusplike feature in the magnetoconductance near the CNP. As mentioned in the Introduction, the gapless edge states are protected from scattering by TRS, which results in a robust ballistic transport. The four-terminal resistance in our samples with a gate size of $18 \times 10 \mu\text{m}^2$, $R_{xx} \simeq 300 \text{ k}\Omega$ is still significantly higher than $h/2e^2$. We have already mentioned above that this discrepancy is not understood. A finite magnetic field breaks down the TRS and the transport of the edge states is strongly suppressed. However, different models predict substantially different physical scenarios.

For example, one of the models predicts that the external magnetic field opens a gap in the edge states dispersion.⁴ The gap is rather small ($E_g \sim 0.3 \text{ meV}$ at $B = 0.1 \text{ T}$), in accordance with theoretical estimations, and conductance should be suppressed in a very narrow interval of the energy when the chemical potential goes through this gap. Experimentally, though, a suppression of conductance is observed in a

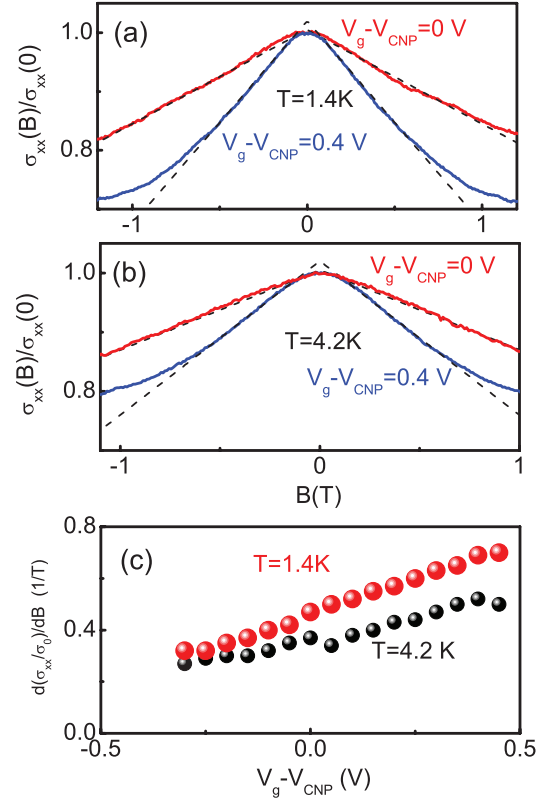


FIG. 4. (Color online) Relative magnetoconductivity for two values of the gate voltage V_g and two temperatures: (a) $T = 1.4$ K and (b) $T = 4.2$ K. Dashed lines are the functions $\sigma_{xx}(B)/\sigma_{xx}(0) = -\alpha|B|$. (c) Parameter $\alpha \approx d[\sigma_{xx}(B)/\sigma_{xx}(0)]/dB$ as a function of the gate voltage for two temperatures: $T = 1.4$ K (large circles) and $T = 4.2$ K (small circles).

much wider interval of the carrier densities, corresponding to the passage of the chemical potential through the bulk gap $E_g \sim 30 \text{ meV}$, in contrast to the theoretical predictions. In Ref. 15 it was predicted that the counterpropagating helical edge states persist in a strong magnetic field. In this model the magnetic field does not create a gap. Instead, it modifies the energy spectrum of the edge states: One of the states merges with the lower bulk Landau level, while the other one remains unchanged. This transformation generates backscattering between the counterpropagating modes in the presence of weak disorder and leads to an increase in the resistance. However, the model¹⁵ does not suggest any realistic description of the scattering and can hardly be compared with experimental observations.

The third model¹⁶ also claims that edge states persist in relatively low magnetic fields, but in magnetic fields above a certain critical B_c , the band structure becomes normal and the system turns into an ordinary insulator. For HgTe devices the critical magnetic field is estimated as $B_c \approx 7.4 \text{ T}$, therefore the resistance increase at fields above 7 T (Fig. 3) can be attributed to the TI–ordinary insulator transition. However, the model cannot explain the growth of the nonlocal resistance at high magnetic field. A similar but somewhat more complicated evolution of the energy spectrum with B has been proposed in Ref. 17.

Finally, a numerical study of the edge state transport in the presence of both disorder and magnetic field has been reported recently in Ref. 18. The authors predict a negative linear magnetoconductance $\frac{\Delta G}{e^2/h} = -A|B|$, where the parameter A strongly depends on the disorder strength W . A physical interpretation of the linear magnetoconductance is given along with the effects analogous to the 1D or 2D antilocalization. We believe that the theoretical model¹⁸ describing the effect of disorder and TRS breaking on the edge transport correctly explains the linear magnetoresistance observed in our experiment. The theory considers two regimes: one corresponding to weak disorder, where $W < E_g$ and the edge states are described by spinless 1D edge liquid, and a strong disorder regime, where $W > E_g$ and the edge states can penetrate deeper into the bulk. Sensitivity to magnetic field strongly depends on which of the two regimes is realized: The parameter A is small for weak disorder and abruptly increases by almost 10–100 times for $W > E_g$. Supposing that the results are valid for a nonballistic case and $A \sim \alpha$, we may conclude that in our samples $W < E_g$. Unfortunately, the precision of the numerical calculations in Ref. 18 does not allow an unambiguous determination of the disorder parameter W from the B slope of the magnetoconductance. It is worth noting that the B slope of the sharp magnetoconductance spike observed in samples with similar size in Ref. 4 is 120 times larger than that in our samples. Admitting that the model¹⁸ is applicable to these data, we obtain the disorder parameter $W \approx 72$ meV, which is almost 2 times larger than the energy gap $E_g = 40$ meV. The disorder parameter W is related to the local deviations of the HgTe quantum well thickness from its average value²⁹ rather than to the random potential due to charged impurities. As has been shown in Ref. 18, the parameter W can be estimated from the value of the mobility. For example, the mobility $\mu \approx 10^5$ cm²/V s corresponds to the momentum relaxation time $\tau = 0.57$ ps, which can be derived from the equation $\tau = \hbar/2\pi v(Wa)^2$, where $a = 30$ Å is the range of the disorder, $v = m^*/\pi\hbar^2$, and m^* is the effective mass. Substituting these parameters into the equation for the relaxation time yields $W = 22$ meV. It is worth noting that the average band gap can be smaller due to the stress. For example, the energy gaps considered in Ref. 29 were $E_g = 14$ meV for the well width $d = 7.3$ nm and

$E_g \approx 20$ meV for $d = 8$ nm. This may explain the difference between our results and those obtained previously in narrow samples.⁴ The fluctuations $W \sim 15$ meV result in a large B slope in wells with $d = 7.3$ nm corresponding to a strong disorder regime in these wells ($W > E_g$) and to a small B slope for wider a well $d = 8$ nm ($W < E_g$).

The physical mechanism behind the linear magnetoconductance cannot be unambiguously identified from the numerical calculations.¹⁸ It is expected that this mechanism is related to a suppression of the interference between closed paths rather than the orbital effect and is analogous to the 1D or 2D antilocalization. The weak temperature dependence observed in our experiments supports this interpretation. The authors claim that for weak disorder the magnetic field has only a perturbative effect on the transport properties of the edge states and expect a quadratic dependence of the magnetoconductance on B rather than a linear one. However, it is not evident from the figures, as has been mentioned by the authors themselves. Further theoretical study will be needed to better understand the mechanism of TRS breaking and the effect of disorder on the edge transport in the QSHE.

In conclusion, we have observed a linear negative magnetoconductance in HgTe-based quantum wells in the QSHE regime where the edge state transport prevails. Our observation agrees with the numerical calculations of the magnetoconductance due to the edge state transport in the presence of nonmagnetic disorder. The B slope of the magnetoconductance is small and corresponds to a weak disorder limit where $W < E_g$ and the magnetoconductance is analogous to a one-dimensional antilocalization. In a magnetic field above 2 T the resistance rapidly decreases and then saturates, which corresponds to the QHE phase. Above 6 T a transition to a high-resistance state is observed, accompanied by a large nonlocal response, which disagrees with the theory.

We thank O. E. Raichev for helpful discussions. Financial support of this work from FAPESP, CNPq (Brazilian agencies), RFBI (Grants No. 12-02-00054 and No. 11-02-12142-ofi-m), and RAS programs “Fundamental Research in Nanotechnology and Nanomaterials” and “Condensed Matter Quantum Physics” is acknowledged.

¹M. Z. Hasan and C. L. Kane, *Rev. Mod. Phys.* **82**, 3045 (2010).

²M. Z. Hasan and J. E. Moore, *Annu. Rev. Condens. Matter Phys.* **2**, 55 (2011).

³X.-L. Qi and S.-C. Zhang, *Rev. Mod. Phys.* **83**, 1057 (2011).

⁴M. König, H. Buhman, L. M. Molencamp, T. Hughes, C.-X. Liu, X.-L. Qi, and S.-C. Zhang, *J. Phys. Soc. Jpn.* **77**, 031007 (2008).

⁵J. Maciejko, T. L. Hughes, and S.-C. Zhang, *Annu. Rev. Condens. Matter Phys.* **2**, 31 (2011).

⁶M. König, S. Wiedmann, C. Brüne, A. Roth, H. Buhmann, L. W. Molenkamp, X.-L. Qi, and S.-C. Zhang, *Science* **318**, 766 (2007).

⁷H. Buhmann, *J. Appl. Phys.* **109**, 102409 (2011).

⁸A. Roth, C. Brüne, H. Buhmann, L. W. Molenkamp, J. Maciejko, X.-L. Qi, and S.-C. Zhang, *Science* **325**, 294 (2009).

⁹G. M. Gusev, Z. D. Kvon, O. A. Shegai, N. N. Mikhailov, S. A. Dvoretzky, and J. C. Portal, *Phys. Rev. B* **84**, 121302(R) (2011).

¹⁰J. E. Moore and L. Balents, *Phys. Rev. B* **75**, 121306 (2007)

¹¹J. E. Moore, *Nature (London)* **464**, 194 (2010).

¹²C. L. Kane and E. J. Mele, *Phys. Rev. Lett.* **95**, 146802 (2005).

¹³B. A. Bernevig and S. C. Zhang, *Phys. Rev. Lett.* **96**, 106802 (2006).

¹⁴B. A. Bernevig, T. L. Hughes, and S. C. Zhang, *Science* **314**, 1757 (2006).

¹⁵G. Tkachov and E. M. Hankiewicz, *Phys. Rev. Lett.* **104**, 166803 (2010).

¹⁶B. Scharf, A. Matos-Abiague, and J. Fabian, *Phys. Rev. B* **86**, 075418 (2012).

¹⁷J.-c. Chen, J. Wang, and Q.-f. Sun, *Phys. Rev. B* **85**, 125401 (2012).

- ¹⁸J. Maciejko, X.-L. Qi, and S.-C. Zhang, *Phys. Rev. B* **82**, 155310 (2010).
- ¹⁹Z. D. Kvon, E. B. Olshanetsky, D. A. Kozlov, N. N. Mikhailov, and S. A. Dvoretzky, *Pis'ma Zh. Eksp. Teor. Fiz.* **87**, 588 (2008) [*JETP Lett.* **87**, 502 (2008)].
- ²⁰G. M. Gusev, E. B. Olshanetsky, Z. D. Kvon, N. N. Mikhailov, S. A. Dvoretzky, and J. C. Portal, *Phys. Rev. Lett.* **104**, 166401 (2010).
- ²¹E. B. Olshanetsky, Z. D. Kvon, N. N. Mikhailov, E. G. Novik, I. O. Parm, and S. A. Dvoretzky, *Solid State Commun.* **152**, 265 (2012).
- ²²S. Das Sarma, S. Adam, E. H. Hwang, and E. Rossi, *Rev. Mod. Phys.* **83**, 407 (2011).
- ²³M. Büttiker, *IBM J. Res. Dev.* **32**, 63 (1988).
- ²⁴H. Jiang, S. Cheng, Q.-f. Sun, and X. C. Xie, *Phys. Rev. Lett.* **103**, 036803 (2009).
- ²⁵J. Maciejko, C. Liu, Y. Oreg, X.-L. Qi, C. Wu, and S.-C. Zhang, *Phys. Rev. Lett.* **102**, 256803 (2009).
- ²⁶A. Ström, H. Johannesson, and G. I. Japaridze, *Phys. Rev. Lett.* **104**, 256804 (2010).
- ²⁷G. M. Gusev, E. B. Olshanetsky, Z. D. Kvon, A. D. Levin, N. N. Mikhailov, and S. A. Dvoretzky, *Phys. Rev. Lett.* **108**, 226804 (2012).
- ²⁸D. A. Abanin, K. S. Novoselov, U. Zeitler, P. A. Lee, A. K. Geim, and L. S. Levitov, *Phys. Rev. Lett.* **98**, 196806 (2007).
- ²⁹G. Tkachov, C. Thienel, V. Pinneker, B. Buttner, C. Brune, H. Buhmann, L. W. Molenkamp, and E. M. Hankiewicz, *Phys. Rev. Lett.* **106**, 076802 (2011).